Photothermal compression of colloidal crystals

Paul A. Rundquist, S. Jagannathan, R. Kesavamoorthy,[a] Charles Brnardic, S. Xu, and Sanford A. Asher[b]
Department of Chemistry, University of Pittsburgh, Pittsburgh, Pennsylvania 15260

(Received 13 July 1990; accepted 17 September 1990)

Dyed sulfonated polystyrene spheres (83 nm diameter) self-assemble into regular crystalline arrays that Bragg diffract visible light. Absorption of high intensity radiation (>25 W/cm^2) by the dye results in a local compression of the crystalline array due to local heating. The Kossel ring pattern is used to probe the variation in the lattice parameter and the dynamics of the thermally induced compression. The thermally induced compression derives from the negative temperature dependence of the interparticle interaction potential.

INTRODUCTION

Aqueous suspensions of charged monodisperse polymer spheres are often used as model systems to study interparticle interactions. Depending upon the sphere charge and number density and the solution ionic strength, these suspensions can show gas, liquid, glass, and crystalline order with macroscopic interparticle separation distances.[1-4] The dominant interparticle interaction derives from a screened Coulomb repulsion between the spheres due to charged groups on their surface. These charges result from ionization of surface functional groups. The repulsive interaction is attenuated by screening of the charges by the diffuse counterion cloud in the medium surrounding the spheres. The repulsive potential decreases monotonically with distance from the sphere surface, and the structural order of the system is determined by such parameters as the sphere diameter, the sphere charge, the particle concentration and the suspension ionic strength. At low ionic strengths ($<10^{-5}$ M) and at sufficiently high particle concentrations, aqueous dispersions of charged polymer spheres will adopt a regular crystal structure in order to minimize the interparticle repulsive interactions.

Colloidal crystals can be prepared with lattice parameters of the order of hundreds of nanometers. These crystals can Bragg diffract radiation in the ultraviolet, visible, and near infrared spectral regions.[5,6] This unique property of colloidal crystals has been used to make practical devices such as a narrow band optical rejection filter.[7,8] Bragg diffraction from the crystals is a sensitive function of the lattice parameter, the sphere diameter, the refractive index mismatch between the spheres and the medium, the crystal Debye–Waller factor and crystal defects.[9,10] Thus, optical diffraction measurements have been extensively utilized to study interparticle interactions in colloidal crystals under shear,[11] gravitational compression[12-14] and in the presence of electric fields, [15] and as a function of temperature.[16-19]

The temperature dependence of the interparticle interaction (and hence the order and stability of a colloidal crystal) derives from the temperature dependence of the dielectric constant of water, the double layer thickness, and the magnitude of the interaction energy relative to the thermal energy. However, until now temperature has not been considered to be a useful variable in the study of interparticle interactions in colloidal crystals because of the limited range of experimentally accessible values. The effects of temperature on colloidal crystals can be strikingly opposite to that observed in atomic and molecular crystals. This difference in behavior occurs because the interparticle interactions depend intimately upon temperature. For example, the repulsive interaction scales with the dielectric constant and the dielectric constant of water decreases faster than $1/T$. In fact, it has been predicted that colloidal crystals will melt upon cooling[20].

In the work discussed in this paper we examine the temperature dependence of colloidal crystalline ordering. We demonstrate that local heating results in a localized compression of the crystal within the heated region. We utilize colloidal spheres containing light absorbing dyes, and we heat the crystal by illuminating it with incident laser light at a wavelength absorbed by the dye. We use Bragg diffraction to dynamically monitor the change in crystal ordering as a function of incident intensity and examine the dynamics of the lattice compression. The dynamics of the crystal compression is determined by the collective motion of the interacting colloidal particles in the crystal.

EXPERIMENTAL

The sulfonated 83 nm ($\pm 5\%$) diameter polystyrene spheres used in this study were synthesized according to procedures which will be described in detail elsewhere. Each sphere contained $\sim 2370 \pm 80$ surface charge groups. The polymer spheres were cleaned by dialysis against deionized water containing Bio-Rad Ag 501-X8 mixed bed ion exchange resin. The dialysis was carried out for 2–4 weeks using 50 000 MWCO Spectra/Por 6 dialysis tubing (Fisher). The dialysis water was changed every 24 h. The cleaned suspensions were stored in Nalgene bottles to minimize contamination from ionic impurities. The ion exchange resin was cleaned using the procedures of Van den Hul and Vanderhoff.[21]

The particle diameter was determined by quasi-elastic light scattering (QELS) using a Langley–Ford 1096 correla-

[a] Also: Materials Science Division, Indira Gandhi Centre for Atomic Research, Kalpakkam 603102, India.
[b] Author to whom correspondence should be addressed.

 0021-9606/91/010711-07$03.00

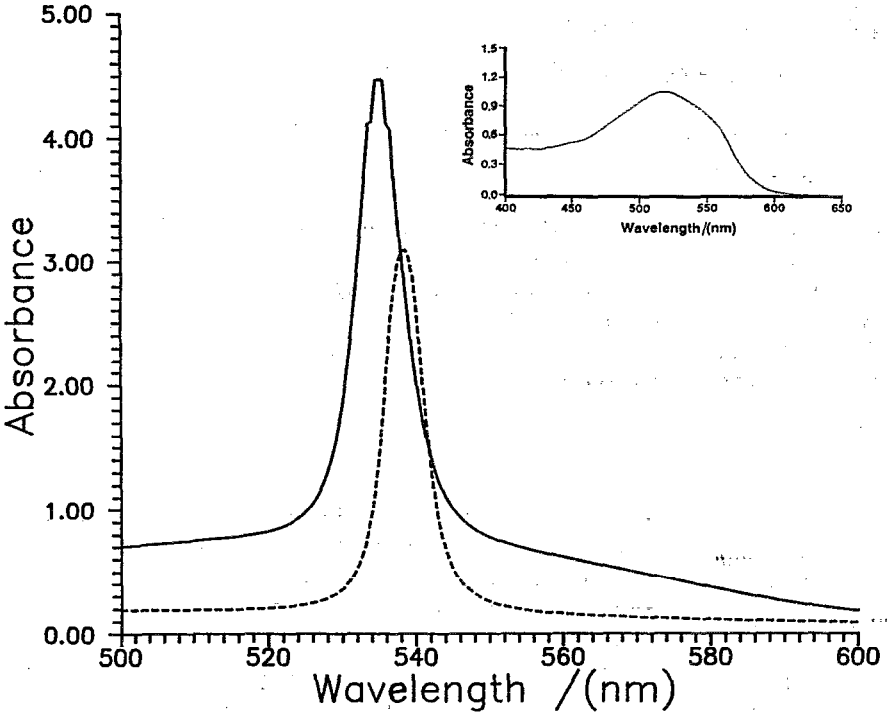

FIG. 1. Visible absorption spectra of the large BCC colloidal crystals prepared from dyed (solid line) and undyed (dashed line) polystyrene spheres. The insert shows the visible absorption spectrum of Oil Red O in ethyl benzene (1.1×10^{-4} M).

tor and confirmed by transmission electron microscopy (TEM). The number of surface charge groups per sphere was determined by measuring the conductivity of the deionized suspension as a function of particle volume fraction[22] using a Radiometer-Copenhagen CDM83 conductivity meter.

The sulfonated polystyrene spheres were dyed with Oil Red O (Aldrich). The insert of Fig. 1 shows the absorption spectrum of the dye in ethyl benzene. The dye was dissolved in acetone, and aliquots of the dye solution were mixed with the cleaned polystyrene suspension. The mixture was agitated for 30–60 min and then dialyzed against deionized water for 2–3 days. Dialysis quantitatively removes the acetone from the suspension mixture. The absorption of the dyed particle suspension was determined to be 30 cm^{-1} at 514.5 nm (for a particle volume fraction of 2%). The particle size and charge did not change upon dye incorporation.

Large body-centered cubic (BCC) crystals of the dyed and undyed 83 nm diameter polystyrene particles were prepared according to published procedures.[7,8] The crystal dimensions were $2.5\times2.5\times0.05$ cm. The sphere volume fraction was maintained at $\sim$2% to remain below the BCC/FCC (face-centered cubic) coexistence region. This was confirmed by the single sharp peak in the diffraction profile of the crystals and the twinned BCC structure Kossel ring pattern.[9] For some of the measurements the crystals were prepared in 0.05 cm quartz cells (NSG Precision Cells). The refractive indices of the suspensions were determined with a temperature controlled Abbe' refractometer (Bausch and Lomb). A Perkin Elmer Lambda 9 UV–Visible–Near IR spectrophotometer was used to obtain transmission spectra of the crystals.

A Spectra Physics Model 164 argon ion laser with a broad band rear reflector was used as the source for the time-dependent intensity measurements. The light was dispersed outside the laser cavity by a diffraction grating and the 514.5 nm beam was reflected by a mirror through a Newport Model 846 HP electronic shutter controlled by a Newport Model 845 digital shutter controller. The shutter, which has a rise time of $\sim$3 ms, determined the minimum temporal pulse width of the pump beam. A 30 cm focal length lens focused the light to a 0.2 mm spot size in the crystal. The 488 nm probe beam was attenuated by neutral density filters and was focused by a 50 cm focal length lens to overlap the pump beam in the sample.

The transmitted probe intensity was detected with a Hamamatsu S1226-18BQ photodiode and the data was collected using a Hewlett–Packard Model 54201A digitizing oscilloscope operating in single shot mode. A narrow bandpass interference filter was placed in front of the photodiode so that only the probe intensity was detected. The electronic shutter triggered the oscilloscope to begin collection.

The samples were oriented such that the transmitted probe beam fell on the inner or outer edge of the projected Kossel ring at the detector resulting in an angle of incidence which was slightly greater than or slightly less than the Bragg angle, respectively. The crystal was allowed to relax for several minutes between measurements at different powers. The Kossel ring oriented about the axis normal to the sample cell derives from BCC (110) planes, and the Kossel

ring diameter depends essentially only upon the lattice parameter. If the probe beam is incident close to the Bragg angle even a small lattice parameter change results in a large change in the transmitted and diffracted intensities.

RESULTS

Figure 1 shows the visible transmission spectra (plotted on an absorbance scale) of the large colloidal crystals prepared with dyed and undyed polystyrene spheres. The insert in Fig. 1 shows the absorption of the dye dissolved in ethyl benzene; this should be essentially identical to the absorption spectrum of the dye within the polystyrene spheres. The transmission of the dyed crystal differs from that of the undyed crystal mainly due to the absorption by the dye. The sharp peaks in Fig. 1 correspond to the transmission minimum for those wavelengths satisfying the Bragg diffraction condition

$$\lambda_0 = 2n_s d_{hkl} \sin(\theta^{xtl}_{hkl}), \quad (1)$$

where λ_0 is the wavelength of incident light in air, n_s is the suspension refractive index, and d_{hkl} is the interplanar spacing of the BCC (110) planes. For normal incidence the Bragg angle in the crystal, θ^{xtl}_{hkl}, is 90°. The spectra were measured by placing the sample cell normal to the light beam of the spectrophotometer. The beam is slightly divergent so the absorption bandwidth partially derives from the angular spread around the 90° nominal incident angle, and the actual attenuation for plane wave incident light ($\sim 10^{-9}$) is much greater than the value measured in the spectrophotometer.[9]

For a given wavelength of light, the incident angles which satisfy the Bragg diffraction condition map as a cone of minimum transmitted intensity, called a Kossel ring, for each set of reflecting planes. The Kossel rings appear as dark circles or ellipses in a diffuse light background when projected on a screen. The diffuse background derives from light scattered by lattice defects and phonons.[9] The pattern of rings on the screen is diagnostic of crystal structure, and the diameter of any ring is related to the lattice parameter for that set of reflecting planes.[23] For a crystal of undyed spheres the Kossel ring diameter is independent of the incident intensity. At low incident intensities (<25 W/cm^2) the diffracted intensities and bandwidths of the crystal of dyed polystyrene spheres are similar to those of the nonabsorbing crystal, while the transmitted intensity is attenuated somewhat by absorption by the dye.[24]

When the incident laser intensity (at 514.5 nm) is increased to above $\sim$25W/cm^2, however, the diffracted and transmitted intensities for the absorbing crystal change appreciably as a function of time. Upon high intensity illumination the Kossel ring decreases in diameter as a function of time, and finally disappears. The rate of contraction of the Kossel ring increases as the incident intensity increases. After the laser beam is turned off the rings reappear and return to their original diameter. The recovery time depends upon the length of time the crystal is exposed to the pump beam.

Photographs and video tapes of the central Kossel ring deriving from the BCC (110) set of planes show 20% Kossel ring diameter changes upon laser heating. This must result from $\sim 6°$ changes in the Bragg angle. In addition, the width of the Kossel ring, measured from the inner edge to the outer edge of the dark ring, increases with time.

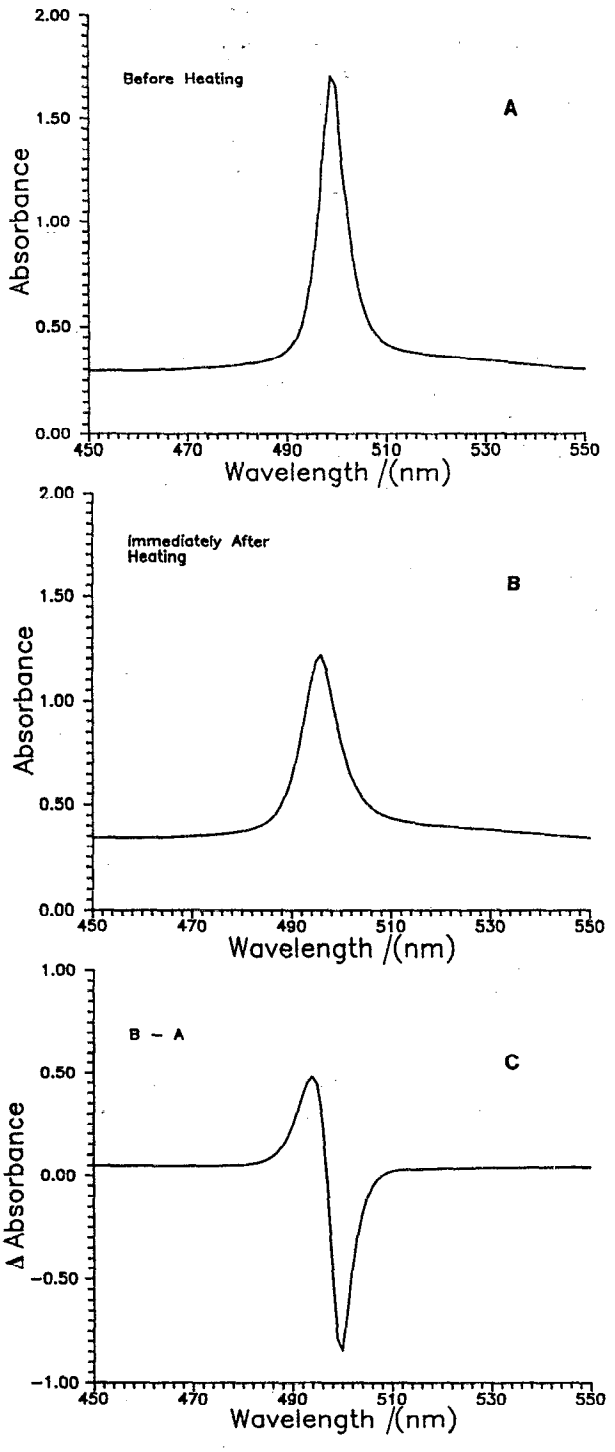

FIG. 2. Visible absorption spectra of an absorbing colloidal crystal in a 0.05 cm pathlength flowcell: (A) before heating, (B) immediately following heating, and (C) the difference spectrum (B)–(A).

Because the diffraction angle and incident wavelength are related by [Eq. (1)], we can also quantitatively measure

the change in the lattice parameter by monitoring the change in the wavelength of the absorption maximum at fixed incident angle using the spectrophotometer. We measured the peak position and bandwidth changes for an absorbing colloidal crystal in a sealed 0.05 cm pathlength quartz cell upon irradiation with 500 mW of 514.5 nm light for 15 min. The incident beam diameter was 4 mm, and a 5 mm diameter circular aperture was placed over the cell to limit the volume sampled in the spectrophotometer to the heated region only. Figure 2 shows the absorption spectra before and ~2 min after heating, and the difference spectrum. The peak position blueshifts by 3 nm immediately after heating. In addition, the peak maximum decreases and the bandwidth increases.

We also measured the transmission through the large BCC crystals of the 488 nm probe during and after heating with the 514.5 nm pump beam. Figure 3 shows the transmission as a function of time where the angle of incidence of the probe beam, θ_i^{air} is ~1.5° greater than the Bragg angle, θ_B^{air} (66°) for the 488 nm probe light. The insert schematically illustrates the geometry of the Bragg and incidence angles relative to the lattice planes. For curve A the crystal was heated for one second with 159 W/cm^2 of 514.5 nm light focused down to 200 μm in diameter. The transmitted probe intensity monotonically decreases while the crystal is heated, and increases exponentially after the pump beam is turned off.

The transmitted intensity decrease is due to the shift of the Bragg condition towards the incident angle of the probe; this is obvious from the Kossel ring contraction upon pump heating. Thus, the light is diffracted away rather than transmitted through the crystal. Upon removal of the pump beam the crystal relaxes and the Bragg angle shifts away from the angle of incidence of the probe beam, and the probe beam transmittance increases. The extent of the transmittance change and the lattice parameter contraction is a function of the extent of crystal heating as shown by curve B in which

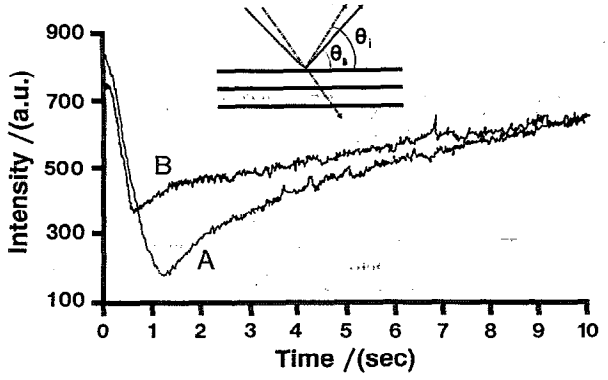

FIG. 3. Probe transmitted intensity as a function of time for the large absorbing crystal with $\theta_i > \theta_B$. (A) The crystal was heated with 159 W/cm^2 for 1 s, and (B) the crystal was heated with 159 W/cm^2 for 500 ms. The insert shows the experimental geometry.

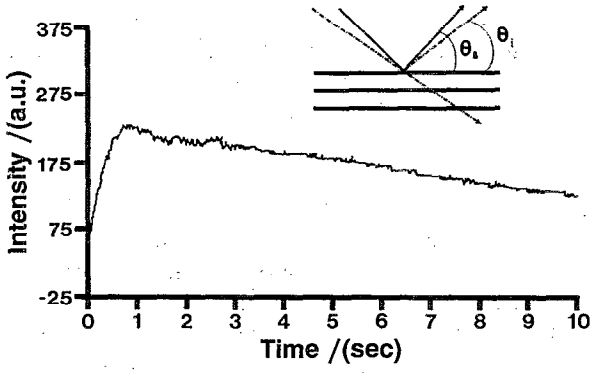

FIG. 4. Probe transmitted intensity as a function of time for the large absorbing crystal with $\theta_i < \theta_B$. The crystal was heated with 382 W/cm^2 for 1 s. The insert shows the experimental geometry.

the pump beam only heats the crystal for 0.5 s compared to the 1 s for curve A.

Figure 4 shows a time-dependent pump/probe measurement where the angle of incidence is slightly less (~1.5°) than the Bragg angle. The pump power flux for this measurement was 382 W/cm^2. The transmitted probe intensity monotonically increases until the pump beam is shut off, then decreases as the crystal relaxes. Here the transmitted intensity increases because the Bragg angle moves away from the pump beam angle of incidence upon heating. When the pump beam is turned off the crystal relaxes resulting in a decrease in the mismatch between the Bragg angle and the angle of incidence, and the transmitted intensity decreases.

Although not clearly shown in Fig. 3 we observe a transmitted intensity increase in a sub 0.1 s timescale when the Bragg angle is less than the angle of incidence. This intensity increase derives from a short time lattice parameter increase which we will discuss in a forthcoming publication.[25]

The temporal changes in the transmitted intensity due to crystal relaxation following the high pump intensity heating appears to follow a single exponential decay. Figure 5 shows a fit to single experimental decay for the data presented in Fig. 3(A). For the case where the angle of incidence is less than the Bragg angle, we also find a clear single exponential decay for the highest pump intensity (382 W/cm^2) data. The single exponential relaxation time constants observed for the large BCC crystals heated by the pump beam for 1 s are listed in Table I.

Undyed BCC colloidal crystals showed no alterations in their diffraction properties upon the pump beam illuminations used in the studies reported above.

DISCUSSION

Absorption of high incident intensities (>25 W/cm^2) of light by a colloidal crystal causes the Kossel rings to contract which indicates an increase in the Bragg angle. This Bragg angle increase is almost entirely due to a decrease in

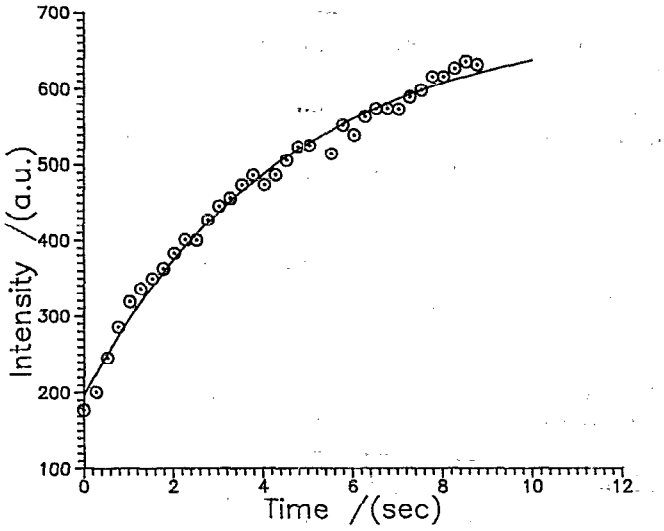

FIG. 5. Exponential fit of the relaxation data in Fig. 3(A). The equation fitted was $y = A + Be^{-t/\tau}$.

the lattice parameter (*vide infra*). The lattice parameter decrease, and the subsequent relaxation after the pump beam is turned off, depends upon the total energy deposited into the crystal. Because the wavelength of the incident light in air is determined by the source and is therefore fixed, the Bragg angle increase derives from a decrease in $n_s d_{hkl}$.

We estimate an upper limit of a $\sim 0.8\%$ decrease in the product $n_s d_{hkl}$ for the pump/probe data presented in this paper. This value is determined by comparing the width of the Kossel ring (measured from the inner to the outer edge of the dark ring) to the Kossel ring diameter. For the measurements where the angle of incidence is slightly greater than the Bragg angle we observe a monotonic decrease in the transmitted probe intensity, until the pump beam is turned off. If the Kossel ring diameter exceeds half of the Kossel ring width then we must observe a decrease in transmittance intensity to a minimum when the Bragg angle equals the angle of incidence. This would then be followed by an increase in transmission as the Bragg angle exceeds the angle of incidence. However, because the observed transmittance decrease is monotonic, the Bragg angle cannot exceed the probe beam incident angle during the pump beam duration. Therefore, we estimate using Eq. (1) that the change in the product $n_s d_{hkl}$ is less than half of the Kossel ring width, or 0.8%.

The temperature dependence of the refractive index of water is well-known, and because the sample consists of only $\sim 2\%$ by volume polystyrene the dependence of the suspension refractive index is essentially identical to that of the water. Because of the similarity to the formation of a thermal lens in an absorbing sample, we used the equation of Dovichi[26] to calculate the thermal equilibration time after the pump beam is turned off for the absorbing colloidal crystals. For an incident beam radius $W = 0.01$ cm and the thermal diffusivity of water (at 20 °C) of $D = 1.42 \times 10^{-3}$ s^{-1} cm^2, the thermal relaxation time is calculated to be 18 ms using the expression $\tau = W^2/4D$. The 18 ms time calculated for thermal equilibration is much faster than the observed relaxation time (of the order of seconds). Thus, the dominant phenomenon giving rise to the change in the Bragg angle is the thermally induced change in the interplanar spacing.

The decrease of the interplanar spacing upon heating derives from the dependence of the interparticle interaction potential on temperature. The interaction potential energy $U(r)$ between two colloidal spheres separated by a distance r can be written as[2]

$$U(r) = \frac{Z^2 e^2}{\epsilon(T)} \left[\frac{e^{\kappa(T)a}}{1+\kappa(T)a}\right]^2 \frac{e^{-\kappa(T)r}}{r}, \tag{2}$$

where Z is the number of charges per sphere, e is the charge of an electron, $\epsilon(T)$ is the temperature-dependent dielectric constant of water, which decreases monotonically with increasing temperature, and a is the sphere radius. The reciprocal Debye double layer thickness $\kappa(T)$ is defined as

$$\kappa^2(T) = \frac{4\pi e^2}{\epsilon(T) k_B T}(n_p Z + n_i), \tag{3}$$

TABLE I. Probe intensity relaxation times (1 s pump duration) for different pump intensities.

	Pump intensity (W/cm^2)	τ(s)
$\theta_i > \theta_B$	159	4.5
	127	6.1
	80	12
$\theta_i < \theta_B$	382	36

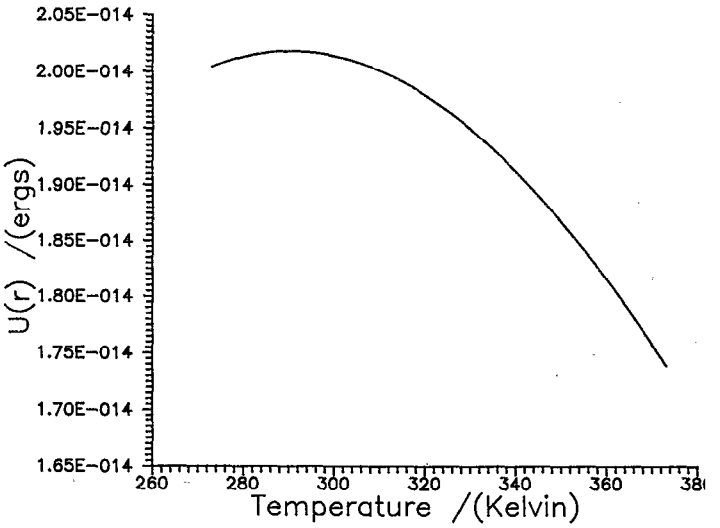

FIG. 6. Plot of the interparticle interaction potential as a function of temperature. The interparticle separation distance is $r = 2.45 \times 10^{-5}$ cm, and the sphere number density is $n_p = 8.85 \times 10^{13}$ cm^{-3}.

where n_p is the particle number density, n_i is the ionic impurity concentration, and $k_B T$ is the thermal energy. We assume that the dissociation equilibrium for the surface strong acid groups is independent of temperature.

Figure 6 shows the temperature dependence of the interaction potential energy between two 83 nm diameter spheres for an interparticle separation distance of 2.45×10^{-5} cm. A renormalized surface charge[27] of $Z = 1150$ charges per sphere was used in this calculation, and the ionic impurity concentration was assumed to be Zn_p. The temperature dependence of the interaction potential energy remains similar if the measured surface charge is used in the calculation. In addition, increasing or decreasing the ionic impurity concentration, which changes the magnitude of the interaction potential energy, will not affect the trend. It is clear that the interparticle repulsive potential decreases with temperature for temperatures above 290 K. Thus, if a small region of the colloidal crystal is elevated in temperature relative to the rest of the sample, the repulsive interactions in this "hot" region will be decreased from that in the surrounding "cold" regions. Therefore, the hot region will be compressed by the surrounding cold regions. Since the hot region is the illuminated region giving rise to the Kossel ring, compression of this region results in a decrease in the average interplanar spacing which decreases the Kossel ring diameter.

In order to estimate how the interparticle separation distance responds to the temperature difference between the heated region and the surrounding colder regions for the absorbing colloidal crystal, we calculated the interaction potential energy as a function of temperature for different values of the interparticle separation distance r while keeping the surface charge, ionic impurity concentration, and the sphere diameter constant. We then calculated the temperature elevation required to achieve identical interaction potential energies for the heated and nonheated regions with their different interparticle separations. Figure 7 plots the relationship of the temperature elevation that accompanies the compression of the interparticle separation in the heated region. From this figure we estimate an upper limit of 30 K for the increase in temperature in the heated region relative to the surroundings when we account for the temperature dependence of the suspension refractive index.

Compression of the colloidal crystal in the region of pump illumination requires that the particle number density n_p increases. Correspondingly, if the particle number density increases in the compressed region, then the regions of the crystal immediately surrounding should show a somewhat larger interplanar spacing as a result of a decreased particle number density. We observed this expansion in regions outside the illuminated volume by translating the crystal following heating and by monitoring the Kossel ring diameter with a low intensity probe beam.

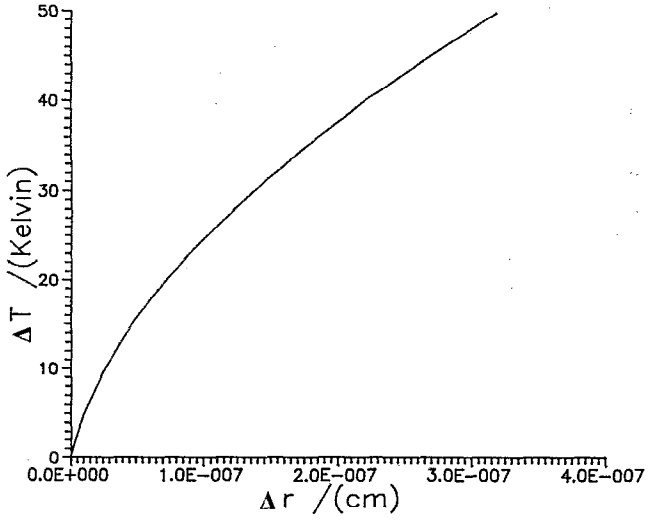

FIG. 7. Plot of the temperature elevation required to maintain identical values of $U(r)$ in the heated and the nonheated regions as the heated region interparticle separation distance is compressed by Δr.

CONCLUSIONS

We show for the first time that the average distance between particles in an electrostatically stabilized colloidal crystal decreases upon local heating. This phenomenon derives from the negative temperature dependence of the interparticle interaction potential. This phenomenon can be used to dynamically control the wavelength of light transmission.

[1] W. B. Russel, D. A. Saville, and W. R. Schowalter, *Colloidal Dispersions* (Cambridge University, New York, 1989).
[2] D. Thirumalai, J. Phys. Chem. **93**, 5637 (1989).
[3] M. O. Robbins, K. Kremer, and G. S. Grest, J. Chem. Phys. **88**, 3286 (1988).
[4] Y. Monovoukas and A. P. Gast, J. Colloid. Interface Sci. **128**, 533 (1989).
[5] P. A. Hiltner and I. M. Krieger, J. Chem. Phys. **73**, 2386 (1969).
[6] S. A. Asher, P. L. Flaugh, and G. Washinger, Spectroscopy **1**, 26 (1986).
[7] S. A. Asher, U. S. Patents Nos. 4 627 689 and 4 632 517.
[8] P. L. Flaugh, S. E. O'Donnell, and S. A. Asher, Appl. Spectrosc. **38**, 847 (1984).
[9] P. A. Rundquist, P. Photinos, S. Jagannathan, and S. A. Asher, J. Chem. Phys. **91**, 4932 (1989).
[10] R. J. Spry and D. J. Kosan, Appl. Spectrosc. **40**, 782 (1986).
[11] B. J. Ackerson, in *Physics of Complex and Supermolecular Fluids*, edited by N. A. Clark and S. Safran (Wiley-Interscience, New York, 1987), p. 553.
[12] R. Kesavamoorthy and A. K. Arora, J. Phys. A Math. Gen. **18**, 3389 (1985).
[13] R. J. Carlson and S. A. Asher, Appl. Spectrosc. **38**, 297 (1984).
[14] R. S. Crandall and R. Williams, Science **198**, 293 (1977).
[15] F. Richetti, J. Prost, and N. A. Clark, in *Physics of Complex and Supermolecular Fluids*, edited by N. A. Clark and S. Safran (Wiley-Interscience, New York, 1987), p. 387.
[16] R. Williams, R. S. Crandall, and P. J. Wojtowicz, Phys. Rev. Lett. **37**, 348 (1976).
[17] J. G. Daly and R. Hastings, J. Phys. Chem. **85**, 294 (1981).
[18] T. Okubo, J. Chem. Soc. Faraday Trans. 1 **82**, 3163 (1986).
[19] T. Okubo, J. Chem. Soc. Faraday Trans. 1 **82**, 3185 (1986).
[20] P. M. Chaiken, J. M. di Meglio, W. D. Dozier, H. M. Lindsay, and D. A. Weitz, in *Physics of Complex and Supermolecular Fluids*, edited by N. A. Clark and S. Safran, (Wiley-Interscience, New York, 1987), p. 321.
[21] H. J. Van den Hul and J. W. Vanderhoff, J. Electroanal. Chem. **37**, 161

(1972).
[22] D. W Schaefer, J. Chem. Phys. **66**, 3980 (1977).
[23] P. Pieranski, Contemp. Phys. **24**, 25 (1983).
[24] P. A. Rundquist, R. Kesavamoorthy, S. Jagannathan, and S. A. Asher, J. Chem. Phys. (in preparation).
[25] R. Kesavamoorthy, S. Jagannathan, P. A. Rundquist, and S. A. Asher, J. Chem. Phys. (submitted).
[26] N. Dovichi, CRC Crit. Rev. Anal. Chem. **17**, 357 (1987).
[27] S. Alexander, P. M. Chaiken, P. Grant, G. J. Morales, P. Pincus, and D. Hone, J. Chem. Phys. **80**, 5776 (1984).